

## Probing the Structure of the Accretion Region in a Sample of Magnetic Herbig Ae/Be Stars

M.A. Pogodin<sup>1</sup>, J.A. Cahuasqui<sup>2</sup>, N.A. Drake<sup>2,3</sup>, S. Hubrig<sup>4</sup>, M. Schöller<sup>5</sup>, M. Petr-Gotzens<sup>5</sup>, G.A.P. Franco<sup>6</sup>, D.F. Lopes<sup>3</sup>, O.V. Kozlova<sup>7</sup>, B. Wolff<sup>5</sup>, J.F. Gonzalez<sup>8</sup>, T.A. Carroll<sup>4</sup>, S. Mysore<sup>5</sup>

<sup>1</sup> *Central Astronomical Observatory at Pulkovo of Russian Academy of Sciences, Pulkovskoye chaussee 65, 196140, Saint-Petersburg, Russia*  
pogodin@gao.spb.ru

<sup>2</sup> *Sobolev Astronomical Institute, St. Petersburg State University, Universitetski pr. 28, 198504, Saint-Petersburg, Russia*

<sup>3</sup> *Observatório Nacional/MCTI, Rua José Cristino 77, CEP 20921-400, Rio de Janeiro, RJ, Brazil*

<sup>4</sup> *Leibniz-Institute für Astrophysik Potsdam (AIP), An der Sternwarte 18, 14482 Potsdam, Germany*

<sup>5</sup> *European Southern Observatory, Karl-Schwarzschild-Str. 2, 85748 Garching, Germany*

<sup>6</sup> *Departamento de Física, ICEX, UFMG, Caixa Postal 702, 30.123-970 Belo Horizonte, MG, Brazil*

<sup>7</sup> *Crimean Astrophysical Observatory, 98409, Nauchny, Crimea, Russia*

<sup>8</sup> *Instituto de Ciencias Astronomicas, de la Tierra y del Espacio (ICATE) 5400, San Juan, Argentina*

**Abstract.** We present the results of a study of the temporal behaviour of several diagnostic lines formed in the region of the accretion-disk/star interaction in the three magnetic Herbig Ae stars HD 101412, HD 104237, and HD 190073. More than 100 spectra acquired with the ISAAC, X-shooter, and CRIRES spectrographs installed at the VLT-8m telescope (ESO, Chile), as well as at other observatories (OHP, Crimean AO) were analyzed. The spectroscopic data were obtained in the He I  $\lambda$ 10830, Pa $\gamma$  and He I  $\lambda$ 5876 lines. We found that the temporal behaviour of the diagnostic lines in the spectra of all program stars can be widely explained by a rotational modulation of the line profiles generated by a local accretion flow. This result is in good agreement with the predictions of the magnetospheric accretion model. For the first time, the rotation period of HD 104237 ( $P_{\text{rot}} = 5.37 \pm 0.03$  days), as well as the inclination angle ( $i = 21^\circ \pm 4^\circ$ ) were determined. Additional analysis of the HARPSpol spectra of HD 104237 and HD 190073, taken from the ESO archive, with the use of the SVD method shows that the magnetic field structure of HD 190073 is likely more complex than a simple dipole and contains a circumstellar component. For the first time, the magnetic field of the secondary component of the binary system HD 104237 was also detected ( $\langle B_z \rangle = 128 \pm 10$  G).

## 1. Introduction

Herbig Ae/Be stars (HAeBes) are pre-main sequence (PMS) objects of intermediate mass approximately from 2 to 8  $M_{\odot}$  (Herbig 1960; Finkenzeller & Mundt 1984; Thé et al. 1994). This corresponds to the range of spectral classes F2 – B0. They are surrounded by dust/gas accretion disks. Remote cold dust reveals itself in the form of a far-IR excess, and numerous emission lines originate in the circumstellar (CS) envelope. This envelope has a complex spatial structure and contains an equatorial accretion disk and matter outflows in the form of a stellar/disk wind at higher latitudes.

One of the important unresolved problems in the HAeBes is the character of the interaction between the accretion disk and the central star. For the lower-mass PMS objects, the classical T Tauri stars (CTTS) with a similar structure of their CS envelopes and strong magnetic fields of the order of kG, the magnetospheric accretion (MA) model is generally recognized. According to this model, the accretion disk does not contact directly the stellar surface, but is truncated by the stellar magnetic field at some distance from the star. A part of the accreted material falls onto the star near magnetic pole regions along the closed magnetic field lines, another part outflows away along the open force lines (Tout & Pringle 1994). However, the HAeBes have weaker magnetic fields (several 100 G). Is the MA model also applicable to them?

If the magnetic axis does not coincide with the rotation axis, a rotational modulation of the line profiles has to be observed with a period  $P$  equal to the rotational period  $P_{\text{rot}}$  of the star. We tried to find signatures of such modulation in the spectra of our program stars.

## 2. Objects of the program

HD 101412 is an early Ae star with an unusually large magnetic field ( $\sim 3$  kG), which is more typical for CTTS than for HAeBes. A magnetic dipole model of the object has been suggested by Hubrig et al. (2011). It ensures a good fitting of observational data, the  $\langle B_z \rangle$  sine-like phase dependency constructed with  $P_{\text{rot}} = 42.078 \pm 0.017^d$  is presented in Fig. 4 of Hubrig et al. (2011).

The second object of our program, HD 104237, is a well-known binary system (A:pe + K) with a T Tauri star as a secondary. The orbital solution of the system has been obtained in Böhm et al. (2004):  $P_{\text{orb}} = 19.859^d$ ,  $e = 0.66$ . The object is the first HAeBe star for which the magnetic field was measured with  $\langle B_z \rangle \approx 50$  G (Donati et al. 1997). Further observations and work by Wade et al. (2007) did not confirm this result, but recently Hubrig et al. (2013) testified the presence of a weak magnetic field ( $\langle B_z \rangle = 63 \pm 15$  G). We can expect that the magnetic field of the object is variable.

The last program object, HD 190073, is a peculiar Herbig A2 IVpe star (Pogodin et al. 2005, and references therein). Its magnetic field ( $\langle B_z \rangle \approx 100$  G) has been measured by various authors (Hubrig et al. 2006, 2009; Catala et al. 2007). There are clear indications of its variability.

## 3. Observations

Three instruments installed at the VLT-8m telescopes (ESO, Chile) were used for spectroscopic observations of the program stars in the near-IR region.

Eight spectra of HD 104237 (March - April 2013) and five spectra of HD 190073 (August - September 2013) were acquired with ISAAC ( $R = 11\,500$ ). 13 spectra of HD 101412 (December 2013 - March 2014), 13 spectra of HD 104237 (November 2013 - January 2014) and six spectra of HD 190073 (March - September 2010) were obtained using X-shooter ( $R \sim 11\,000$ ). These spectra cover a wide spectral range from the near-UV to the near-IR and also include the He I  $\lambda 5876$  line. Nine additional spectra of HD 101412 (April 2011 - March 2013) were acquired with CRIRES ( $R = 110\,000$ ). The  $S/N$  ratio of all spectra was between 200 and 400.

Additionally, 51 spectra of HD 190073 near the He I  $\lambda 5876$  line were collected from archives of several observatories (ESO, OHP, Crimean AO), which were obtained between 1994 and 2013 (Pogodin et al. 2005, 2012; Kozlova 2014).

#### 4. Results of the observations

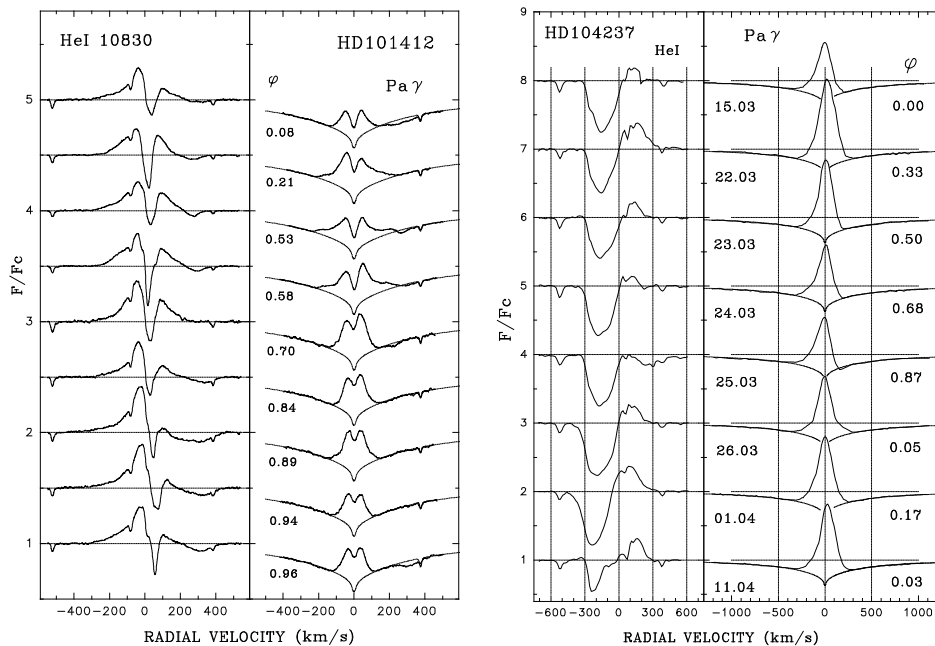


Figure 1. *Left:* Typical profiles of the IR He I  $\lambda 10830$  and Pa  $\gamma$  lines in the spectrum of HD 101412. Phases of  $P_{\text{rot}} = 42.076^{\text{d}}$  are indicated. *Right:* The same as in the left panel but for HD 104237 and  $P_{\text{rot}} = 5.37^{\text{d}}$ .

Typical profiles of the two IR lines He I  $\lambda 10830$  and Pa  $\gamma$  in the spectra of HD 101412 (CRIRES) and HD 104237 (ISAAC) are shown in Fig. 1. The emission He I line profile of HD 101412 has two redshifted absorption components. One is wide, shallow, and strongly redshifted. The second is narrow, deep and with a weak red shift. The emission profile of the Pa  $\gamma$  line is a single one with a central absorption. The profiles of these two IR lines in the spectrum of HD 104237 demonstrate quite different types. The He I line profiles are of P Cyg type, which is evidence for a strong stellar wind and an intermediate orientation of the rotation axis relative to the line of sight. The Pa  $\gamma$  line does not show signs of wind. Its density is not enough to be visible in this subordinate

line. As in the case of HD 104237, HD 190073 has similar IR line profiles: He I  $\lambda 10830$  with a P Cyg structure and Pa $\gamma$  with a single emission profile. This object has also an intermediate orientation relative to the observer. The He I  $\lambda 5876$  line profiles appear as single emissions too.

## 5. Analysis of the results

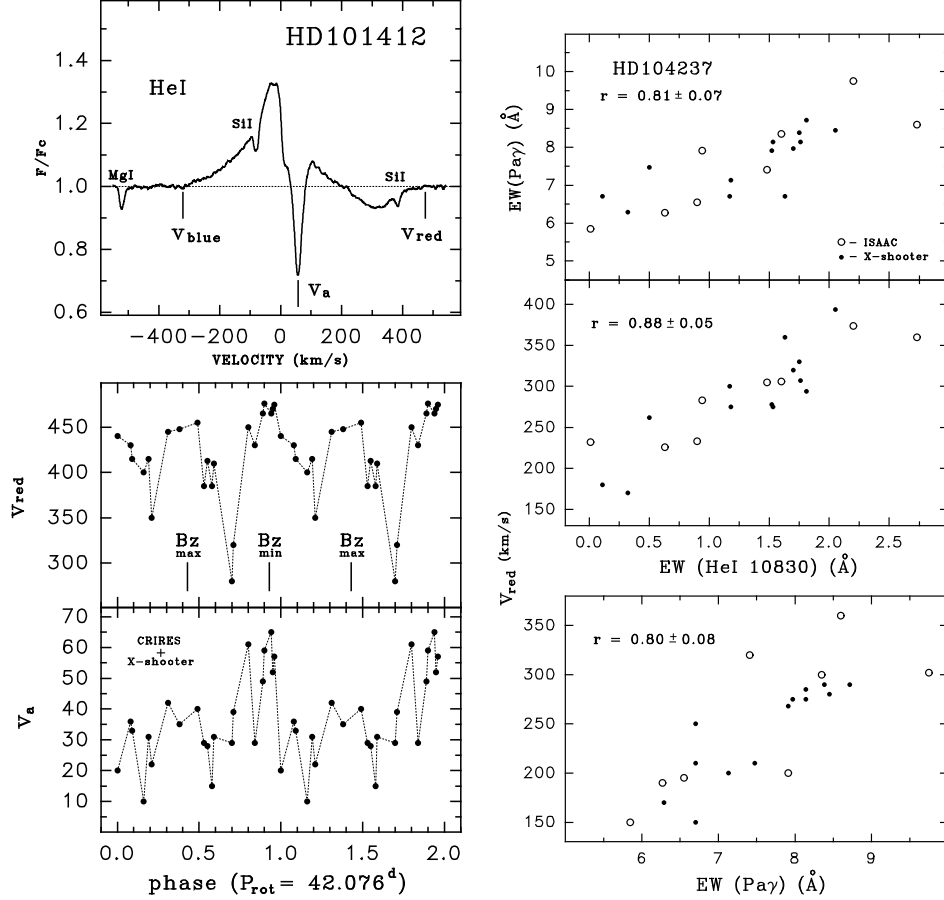


Figure 2. *Left:* Phase dependencies of the velocities  $v_{\text{red}}$  and  $v_a$  of the He I  $\lambda 10830$  profile in the spectrum of HD 101412. *Right:* Dependencies between different parameters of the IR lines in the spectrum of HD 104237.  $EW$  of the Pa $\gamma$  line and  $v_{\text{red}}$  velocity versus  $EW$  of the He I 10830 line (top and middle panels respectively);  $v_{\text{red}}$  versus  $EW$  of the Pa $\gamma$  line (bottom panel). In the measurements of  $EW$  of the emission component of the He I  $\lambda 10830$  line, we considered emission above the underlying continuum, whereas in the case of the Pa $\gamma$  line, the  $EW$  of the emission component was measured as an emission above the preliminary calculated photospheric Pa $\gamma$  absorption profile.

The model of the magnetic dipole-type field of HD 101412 (Hubrig et al. 2011) suggests that the angle between the rotation axis and the line of sight is  $i = 80^\circ \pm 7^\circ$ , and the angle between the rotation and magnetic axes is  $\beta = 84^\circ \pm 13^\circ$ . With such an

orientation, the magnetic axis has to be located close to the disk plane. The MA model predicts two flows of material falling down onto each magnetic pole region. During one period, two episodes of velocity increase towards the star should be observed. Fig. 2 (*left*) illustrates the temporal behaviour of the different parameters of the He I  $\lambda 10830$  profile depending on the phase of  $P_{\text{rot}} = 42.078^{\text{d}}$ . This quasi-resonance line is formed in the high-temperature regions ( $T_e \geq 15\,000$  K) including the innermost disk and the two accretion flows. The velocity  $v_a$  (Fig. 2, *top left*) characterizes the kinematics at the disk, and the velocity  $v_{\text{red}}$  the kinematics at the flows. One can see in Fig. 2 (*bottom left*), that  $v_{\text{red}}$  reaches its maxima twice per period exactly at the phases where  $\langle B_z \rangle$  has the positive and negative extrema (see Hubrig et al. 2011, Fig. 4). These are the phases when the magnetic poles cross near the line of sight. The behaviour of  $v_a$  is similar, but with a smaller amplitude: the accretion process from the innermost disk is just beginning. The Pay line is formed over a more extended region of the disk, and the accretion flows in this line are less noticeable. The behaviour of the He I line parameters fully confirms the MA model predictions.

Unlike HD 101412, the line profiles of HD 104237 do not show absorption related to the accretion flow (apart from March 25, 2013), see Fig. 1 (*right*). However, screening of the stellar limb by the accretion flow appears as a depression in the red wing of the emission profile: the velocity of the red wing edge  $v_{\text{red}}$  and the equivalent width  $EW$  decrease. Fig. 2 (*right*) shows that variations of these parameters for both IR lines have a notable correlation. Unlike  $v_{\text{red}}$ , the velocity of the blue wing edge  $v_{\text{blue}}$  of these lines does not correlate with  $EW$ . This confirms our assumption that the depression of the profile red wing is linked to the flow passing across the line of sight.

We tried to determine the rotation period,  $P_{\text{rot}}$ , of HD 104237 using a method based on fitting phase dependencies for each value of the trial period  $P$  with a sinusoid for a wide range of  $P_{\text{rot}}$  (3.8 – 6.8 days) with a step width of  $0.001^{\text{d}}$ . The parameters of the sinusoid, such as amplitude  $A$ , constant coefficient  $C$ , and initial phase  $\varphi_o$  were determined using a standard Least-Square method for each value of  $P_{\text{rot}}$ . Fig. 3 (*left*) illustrates the periodograms calculated for the parameter  $EW$  of the Pay line, where  $\sigma$  is the standard deviation of values from the sine line. We calculated also the periodogram for the parameter  $\sigma_{\text{fr}}$  which is the mean square value of the fractional remainder after dividing all time intervals between neighboring observations by a trial period  $P_{\text{rot}}$ . If the intervals are close to an integer number of  $P_{\text{rot}}$ , then  $\sigma_{\text{fr}}$  is close to zero. In our case we have found  $P_{\text{rot}} = 5.37^{\text{d}}$  for the parameter  $EW$  of the Pay line and have been convinced that this value does not correspond to a minimum of the parameter  $\sigma_{\text{fr}}$ . Therefore, our estimation of  $P_{\text{rot}}$  is not a result of the sampling dates. We plotted periodograms for parameters  $EW$  and  $v_{\text{red}}$  for the lines He I  $\lambda 5876$ ,  $\lambda 10830$  and Pay: for ISAAC data (8 dates), X-shooter data (13 dates), and all of the dates together (21 dates). The total number of obtained periodograms was 14, the parameters of the sinusoid  $A$  and  $\varphi_o$  were determined for each case. After averaging, the results were:  $P_{\text{rot}} = 5.37^{\text{d}} \pm 0.03^{\text{d}}$ ,  $\varphi_o = 0.030 \pm 0.041$ . The phase dependencies of the parameters  $EW$  and  $v_{\text{red}}$  for different lines in the spectrum of HD 104237 are illustrated in Fig. 3 (*right*). Using standard formulas, we derived the inclination angle  $i$ . Several estimations of the stellar radius  $R_*$  were given in Fumel & Böhm (2012) with a mean value of  $2.95 \pm 0.11 R_{\odot}$ . The following values of  $v \sin i$  were published in different papers:  $12 \pm 2 \text{ km s}^{-1}$  (Donati et al. 1997),  $10 \pm 1 \text{ km s}^{-1}$  (Acke & Waelkens 2004), and  $8 \pm 1 \text{ km s}^{-1}$  (Cowley et al. 2013). Adopting  $v \sin i = 10 \pm 2 \text{ km s}^{-1}$ , we derived  $i = 21^{\circ} \pm 4^{\circ}$ .

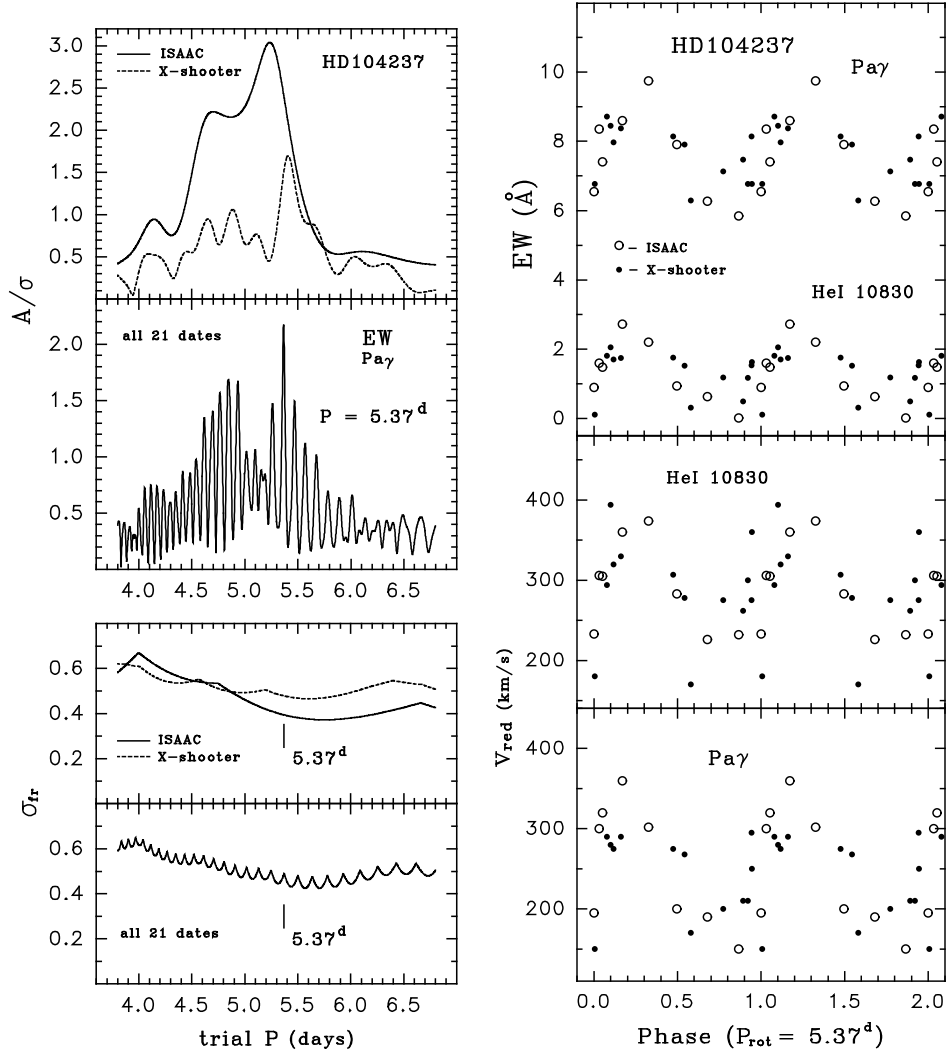


Figure 3. *Left:* Periodograms for  $EW$  variations of the Pay line in the spectrum of HD 104237. *Right:* Phase dependencies of the parameters  $EW$  and  $v_{red}$  in the spectrum of HD 104237.

For HD 190073, we had only 11 spectra in the IR region in the period 2010 – 2013, which was not enough for a detailed study. The analysis of 51 optical spectra near the He I  $\lambda 5876$  line showed the presence of a large-amplitude variability on the timescale from 1 day to several years. We separated two main types of this variability, which is illustrated in Fig. 4 (*left*): *a*) a global change of intensity of the line without variations in the shape of the profile (type I), and *b*) a distortion of the red wing of the emission profile, as also observed for HD 104237 (type II). Fig. 4 (*right*) shows the correlations of  $v_{red}$  and  $v_{blue}$  with the  $EW$  of the line. In the case of the  $v_{blue}/EW$  dependency, a notable but rather weak correlation is observed ( $r = -0.56 \pm 0.10$ ). This correlation corresponds to the type I variability. The  $v_{red}/EW$  correlation is much stronger ( $r = 0.81 \pm 0.05$ ), it corresponds to both variability types I and II. We can see

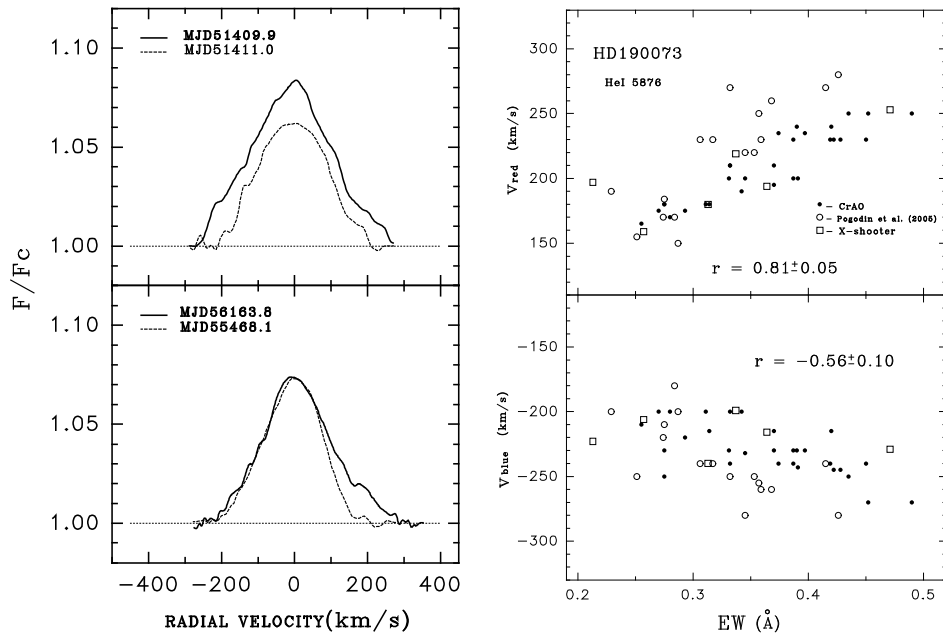


Figure 4. *Left:* Two types of the He I  $\lambda 5876$  line profile in the spectrum of HD 190073. *Right:* Correlations of the velocities  $v_{\text{red}}$  and  $v_{\text{blue}}$  with  $EW$  of the He I  $\lambda 5876$  line profile in the spectrum of HD 190073.

that the contribution of the type II variability is rather strong in the global behavior of the He I  $\lambda 5876$  line profile variations in the spectra of HD 190073. Unfortunately, other attempts to exactly determine the  $P_{\text{rot}}$  of HD 190073 were not successful. However, the behaviour of the  $v_{\text{red}}/EW$  parameter confirms (as in the case of HD 104237) our assumption of a rotating accretion flow that distorts the red wing of the emission He I  $\lambda 5876$  profile. We assume that the magnetic field configuration of HD 190073 can be more complex than a simple dipole, and the whole picture of spectral variability is less simple.

Magnetic field measurements were done using high-resolution spectra of HD 104237 and HD 190073 obtained using the HARPS instrument in polarimetric mode, installed at the 3.6-m ESO telescope (Chile) and retrieved from the ESO archive. We used the multiline Singular Value Decomposition (SVD) method for Stokes Profile Reconstruction (Carroll et al. 2012). For HD 104237, we can see polarization features corresponding to the primary component (rather marginal) and to the secondary component of this binary system (Fig. 5, *left*). The latter is quite notable with  $\langle B_z \rangle = 128 \pm 10$  G. This is the first discovery of the magnetic field of the secondary of HD 104237. Another situation is found for HD 190073. Instead of one polarization feature corresponding to the SVD absorption line, we see two features of opposite signs centered at emission wings around the central absorption (Fig. 5, *right*). It is possible that the CS component has a significant contribution to the general configuration of the magnetic field of HD 190073.

**Acknowledgments.** This work was supported by the Basic Research Program of the Presidium of the Russian Academy of Sciences P-21 “Non-stationary phenomena in objects of the Universe”. N.A.D. acknowledges the support of the PCI/MCTI grant

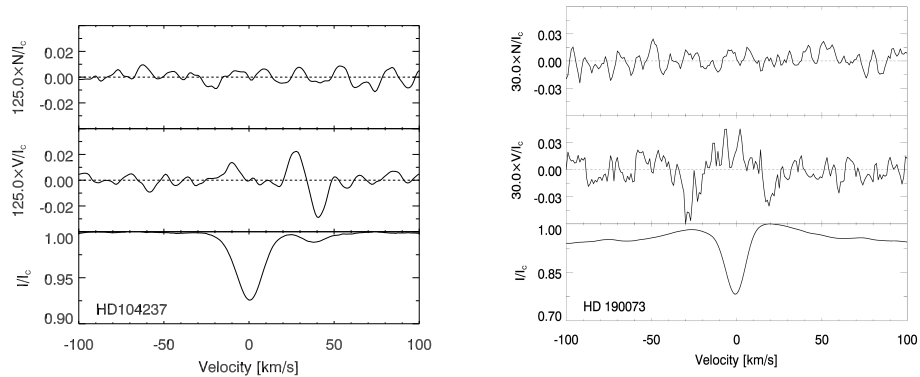


Figure 5. SVD spectra of HD 104237 and HD 190073 obtained on May 3, 2010 and August 7, 2012, respectively. The upper spectra represent the diagnostic null spectra, which are associated with the Stokes  $V$  spectra by using subexposures with identical waveplate orientation. Below the null spectra, we present the Stokes  $V$  and Stokes  $I$  spectra. The  $V$  and null profiles were expanded by a factor of 125 and 30 for HD 104237 and HD 190073, respectively, and shifted upwards for better visibility.

under the project 302350/2013-6 and the St. Petersburg State University for research grant 6.38.18.2014. We would like to thank I. Ilyin for fruitful discussions on the rotation periods.

## References

- Acke B., Waelkens C., 2004, *A&A*, 417, 1009  
 Böhm T., Catala C., Balona L., Carter B., 2004, *A&A*, 427, 907  
 Carroll T.A., Strassmeier K.G., Rice J.B. et al., 2012, *A&A*, 548, A95  
 Catala C., Alecian E., Donati J.-F. et al., 2007, *A&A*, 462, 293  
 Cowley C.R., Castelli F., Hubrig S., 2013, *MNRAS*, 431, 3485  
 Donati J.-F., Semel M., Carter B.D. et al., 1997, *MNRAS*, 291, 658  
 Finkenzeller U., Mundt R., 1984, *A&AS*, 55, 109  
 Fumel A., Böhm T., 2012, *A&A*, 540, 108  
 Herbig G.H., 1960, *ApJS*, 4, 337  
 Hubrig S., Yudin R.V., Schöller M. et al., 2006, *A&A*, 446, 1089  
 Hubrig S., Stelzer B., Schöller M. et al., 2009, *A&A*, 502, 283  
 Hubrig S., Mikulášek Z., Gonzalez J.F. et al., 2011, *A&A*, 525, L4  
 Hubrig S., Ilyin I., Schöller M., Lo Curto G., 2013, *AN*, 334, 1093  
 Kozlova O.V., 2014, *Astrophysics*, *in preparation*  
 Pogodin M.A., Franco G.A.P., Lopez D.F., 2005, *A&A*, 438, 237  
 Pogodin M.A., Hubrig S., Yudin R.V. et al., 2012, *AN*, 333, 594  
 Thé P.S., de Winter D., Perez M.R., 1994, *A&AS*, 104, 315  
 Tout G.A., Pringle J.E., 1994, *MNRAS*, 281, 219  
 Wade G.A., Bagnulo S., Drouin D. et al., 2007, *MNRAS*, 376, 1145